Available online at www.sciencedirect.com
SCIENCE DIRECT®
ELSEVIER
Nuclear Instruments and Methods in Physics Research A 532 (2004) 357–365
NUCLEAR INSTRUMENTS & METHODS IN PHYSICS RESEARCH Section A
www.elsevier.com/locate/nima

Electron cooling experiments at the ESR

M. Steck*, P. Beller, K. Beckert, B. Franzke, F. Nolden

GSI, Gesellschaft für Schwerionenforschung, Planckstraße 1, D-64291 Darmstadt, Germany

Available online 28 July 2004

Abstract

The properties of electron cooled beams of highly charged ions have been studied at the ESR. New experiments using a beam scraper to determine the transverse beam size provide the beam parameters in the intrabeam scattering dominated intensity regime, but also at very low intensity when the ion beam enters into an ultra-cold state. Extremely low values of longitudinal and transverse beam temperature on the order of meV were achieved for less than 1000 stored ions. An experiment with bunched ultra-cold beam showed a limit of the line density which agrees with the one observed for coasting beams. Cooling of decelerated ions at a minimum energy of 3 MeV/u has been demonstrated recently.

PACS: 29.20.Dh; 29.27.Bd; 41.75. – i

Keywords: Highly charged ions; Storage ring; Electron cooling; Beam ordering

1. Introduction

The electron cooling system of the ESR storage ring was designed as a multi-purpose device which can be utilized in various modes of operation of the storage ring [1]. Continuous electron cooling is applied to the stored ion beam for the compensation of the heating by an internal gas jet target [2]. Radioactive beams are cooled to ultimate momentum spread for precision mass spectrometry [3]. During operation of the RF system, electron cooling supports the capture into RF buckets and consequently increases the bunching efficiency. Particularly for deceleration of highly charged ions electron cooling is crucial in order to increase the efficiency and to compensate the adiabatic growth of the phase space volume [4]. The most important feature is the ability to cool beams to highest quality for experiments with stored highly charged ions. Electron cooling is most powerful when the injected ion beam has small emittance and momentum spread. For hot beams, like radioactive ion beams, electron cooling is supported by stochastic pre-cooling, which allows a considerable reduction of the total cooling time [5].

2. Present parameters of the ESR electron cooling system

The ESR electron cooling system is operated basically as it was originally designed [6], only a

*Corresponding author. Tel.: +49-6159-71-2406; fax: +49-6159-71-2785.
E-mail address: m.steck@gsi.de (M. Steck).

0168-9002/$ - see front matter © 2004 Elsevier B.V. All rights reserved.
doi:10.1016/j.nima.2004.06.065

few minor modifications and improvements were made in the course of time. The electron beam is generated from a 50.8 mm diameter cathode immersed in a longitudinal magnetic field which guides the electron beam from the gun to the cooling section and to the electron collector in a constant field strength. At higher electron energies a field strength around 0.1 T is chosen. In recombination experiments field strengths up to 0.18 T have been employed [7], whereas at the lowest electron energies for cooling of decelerated highly charged ions the field strength is reduced down to 0.015 T.

Electron energy and electron current can be set independently. Electron energies in the range from 1.6 to 230 keV have been used for the cooling of ion beams. The highest accelerating voltage which has been applied to gun and collector after extensive conditioning is 265 kV. The maximum voltage is limited by the time spent on the conditioning process. Electron currents up to 1 A have been applied for cooling in situations when the cooling time had to be minimized. For best stability and quality of the cooled ion beam an electron current of a few hundred milliamperes is used. Around 0.5 A instabilities caused by trapping of residual gas ions set in causing energy fluctuations of the electron beam and consequently of the cooled ion beam. An electron current of a few milliamperes can be sufficient for cooling, particularly for low-energy beams when the electron density is increased due to the reduced velocity.

A low vacuum pressure in the electron cooler is crucial for stable operation for two main reasons. Firstly, discharges in the gun and collector sections which have electric and magnetic fields perpendicular to each other are disappearing with decreasing vacuum pressure. Secondly, the production and capture rate of residual gas ionization products is reduced and they can be cleared by transverse electric fields more easily. The basic pressure in the electron cooler is 3×10^{-11} mbar. Heating of the cathode does not significantly deteriorate the pressure. Under electron beam operation the electron loss current to ground determines the vacuum pressure, the pressure increases proportionally to the electron loss current. Even at maximum electron currents the pressure does not exceed 1×10^{-10} mbar, if the electron losses are carefully minimized.

3. Electron cooled beams in equilibrium with intrabeam scattering

Electron cooling in a storage ring is primarily applied to provide ion beams of ultimate quality for experiments performed on the stored ion beam. The main limitation for intense ion beams does not originate from the temperature of the electron beam which sets a lower limit to the achievable ion beam temperature. The dense ion beam provided by electron cooling is subject to Coulomb collisions which result in an exchange of thermal energy between the degrees of freedom called intrabeam scattering. As the beam energy is many orders of magnitude higher than the internal thermal energy, the transfer of energy from the longitudinal energy into internal motion is the main source for the heating of the internal motion. The reduction of the phase space volume by electron cooling is inevitably linked to a growth of the heating rate by intrabeam scattering which grows inversely proportionally to the phase space volume of the ion beam. If the ion current exceeds a value of about 5 mA coherent transverse oscillations arise. They can be remedied, to some extent, by feedback systems. For most experiments performed at the ESR such high ion beam intensities are not requested.

The systematic variations of the beam parameters, longitudinal momentum spread and transverse emittances, have been investigated before [8]. The experiments evidenced an increase of the phase space volume with the number of stored ions N when a constant electron current was applied. The momentum spread $\delta p/p$ increased with $\delta p/p \propto N^{0.3}$, the transverse emittances $\varepsilon_{x,y}$ with $\varepsilon_{x,y} \propto N^{0.6}$. The total phase space volume thus increased proportionally to $N^{1.5}$. This more than linear increase was attributed to a reduction of the cooling rate which is a consequence of the increasing relative velocities between ions and electrons when the phase space volume increases. In these experiments the momentum spread was

determined by Schottky noise analysis, the emittances were derived from beam profiles which were measured employing particle detectors for ions which have captured an electron in the cooler and which are separated from the circulating primary beam in the bending sections of the storage ring [9].

More recently similar studies of the beam emittance have been performed employing a beam scraper to determine the transverse beam size. The beam scraper position can be changed in steps of 5 μm, the reproducibility of the positioning is better than 20 μm. The beam size is determined as the difference between the position where the ion beam is destroyed completely and the position where a certain number of particle survives after the scraper has been moved to this position. For intense beams the beam radius determined by scraping agrees well with non-destructive diagnostics employing a residual gas ionization beam profile monitor (Fig. 1). The profile monitor measurement is corrected according to the square root of the ratio of the beta-function values at the two positions in the ring. The comparison between the two methods shows that the scraper method corresponds to about 3 times the rms radius measured with the beam profile monitor. For lack of a vertical beam profile monitor the vertical size can only be calibrated against a particle detector,

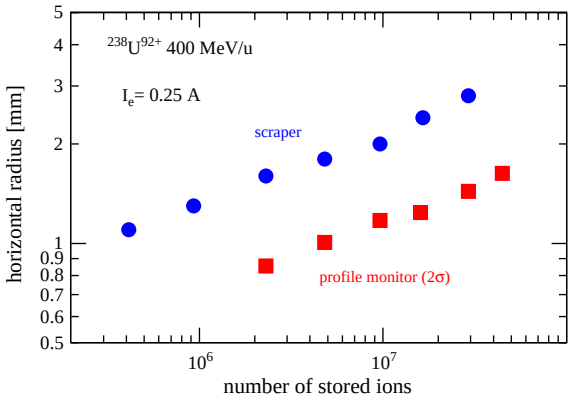

Fig. 1. Comparison between the beam radius determined by the scraper and the 2σ-value measured non-destructively with a beam profile monitor. The beam width at the profile monitor is corrected for the difference of the ion optical β-function in the two positions.

which confirms the comparison for the horizontal beam size.

The measurement of the beam size and the momentum spread as a function of the number of stored ions for different ion species with the scraper (Fig. 2) shows a similar systematic dependency as previously observed with particle detectors [10]. The emittance and momentum spread increase proportionally to $N^{\kappa,\lambda}$, respectively, with an exponent $\kappa = 0.5$–0.6 for the emittance and $\lambda = 0.26$–0.30 for the momentum spread. The values are slightly lower than in the previous measurements. This can be attributed to improvements of the cooling rate, but might also be caused by the resolution of the detection technique. The phase space density of the cooled beam decreases weakly with the number of stored ions, the phase space density is proportional to $N^{-\mu}$, with μ in the range 0.3–0.6.

The measurements show a weak dependence on the ion species. The heating rate by intrabeam scattering is proportional to q^4/A^2, whereas the cooling rate for cold beams approximately increases proportionally to $q^{1.5}/A$ [11]. Consequently, the phase space density of the ion beam should decrease with $(q^{2.5}/A)^{-1}$, in reasonable agreement with the measurements.

4. Beam parameters of low-intensity ultra-cold beams

At low ion beam intensities it was observed that intrabeam scattering is suppressed and the beam enters into an ultra-cold state with extremely low temperature. This was evidenced by a sudden reduction of the momentum spread when the number of stored ions is reduced to less than 1000 [12]. In the longitudinal degree of freedom momentum spreads as low as $\delta p/p = 1 \times 10^{-7}$ can be easily resolved by Schottky noise analysis. For the transverse degree of freedom observation of a similar effect of emittance reduction was ruled out by the resolution of the non-destructive detectors which is about 1 mm.

Beam scraping allows a significantly improved resolution for the transverse beam size, however, at the expense of beam destruction. Particularly

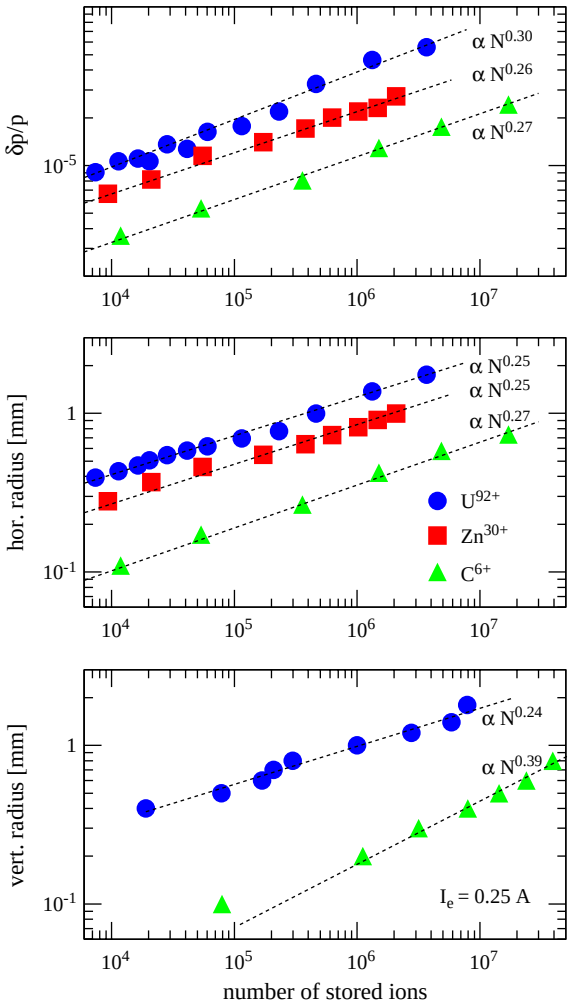

Fig. 2. Momentum spread and beam radius for three ions (C^{6+}, Zn^{30+}, U^{92+}) at an energy of 400 MeV/u cooled by an electron current of 0.25 A. The dependence of the beam parameters on the beam intensity is a result of an equilibrium between cooling and intrabeam scattering. The fit values for the power-law increase of the beam parameters with particle number N are given.

for the horizontal beam size the resolution can be on the order of micrometers. This resolution is achieved by transverse displacement of the ion beam in a dispersive section of the storage ring, instead of the less accurate positioning of the scraper [13]. The transverse ion position is controlled by minute changes of the electron energy which result in corresponding changes of the ion beam energy. The value of the horizontal position change is determined by the dispersion value at the scraper location. Due to the vanishing vertical dispersion, this technique is not applicable to vertical beam size measurements and the vertical beam size can only be determined by mechanical movement of the scraper.

The measurement of the horizontal beam size of the low-intensity beam by small changes of the beam energy evidenced a similar reduction of the beam size as observed before for the momentum spread. The Schottky noise was measured for varying distance between the beam center and the scraper edge. The noise power of the 21st harmonic of the revolution frequency and the momentum spread determined from the frequency spread $\delta f/f$ according to $\delta p/p = \eta^{-1}\delta f/f$ with the frequency slip factor η are shown in Fig. 3 as a function of the scraper position. The measurement starts with an ion beam orbit which lies further inside than the scraper edge. Then the distance of the beam center to the scraper is reduced step-by-step, until the beam is destroyed completely. The point of complete beam loss is the center of the beam. The noise power decreases continuously when the beam approaches the scraper from the inside. At the position when the momentum spread drops by one order of magnitude the noise power stays constant. Just before the transition the signal-to-noise ratio is lowest, but even then the beam signal exceeds the electronic noise by an order of magnitude. As the beam noise power is proportional to the number of ions, the beam intensity is not further reduced by the scraper. This can be explained by a discontinuous reduction of the horizontal beam size similar to that of the momentum spread. The ion beam disappears suddenly when the beam position is changed by less than 5 μm.

The comparison of two separate measurements in Fig. 3 shows a very good reproducibility of the method. The transition from the intrabeam scattering dominated beam to the ultra-cold beam occurs for the same scraper position. The values for the momentum spread are well reproduced, except the small momentum spread values for which it is known that the Schottky signal width is broadened by fluctuations of the bending field strength due to power supply ripple.

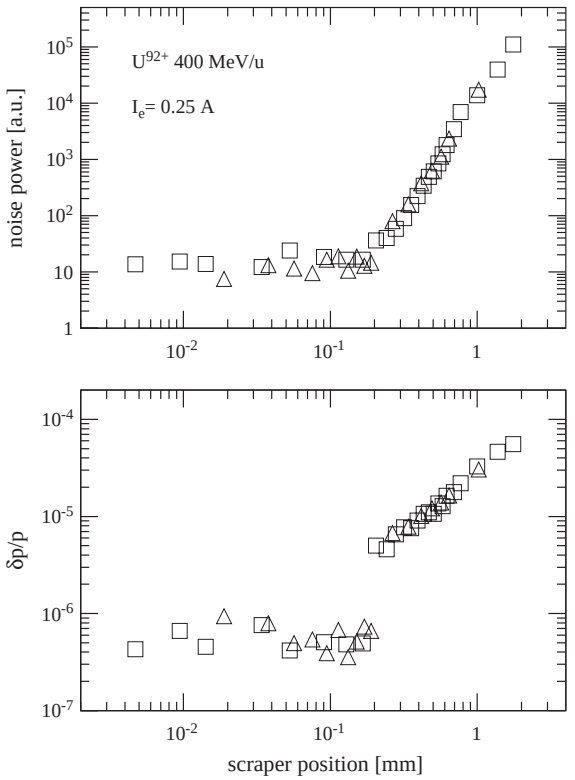

Fig. 3. The noise power and the momentum width of the beam as a function of the scraper position for bare uranium ions at 400 MeV/u. The beam intensity is reduced by bringing the beam center closer to the scraper. At a distance of 0.2 mm the momentum spread drops and the scraper does not reduce the beam intensity any further.

The behavior of the beam size at the transition point from the intrabeam scattering dominated regime to the ultra-cold state confirms the hypothesis of the existence of an ordered state. Due to vanishing intrabeam scattering the ion beam is cooled to the electron beam temperature and the ions line up in a linear string with negligible transverse oscillations about the closed orbit. The momentum spread of the ion beam is limited by the longitudinal electron temperature.

The new method to measure the beam size and consequently the beam emittance allows the investigation of a dependence on the particle species. For intensities exceeding 10^6 stored ions the intensity can be measured with a beam current transformer. For lower intensities the integrated noise power in one harmonic of the revolution frequency is used to measure the beam intensity. The Schottky noise power is calibrated at higher intensity versus the current transformer. Noise suppression of the Schottky signal due to collective effects is negligible as confirmed by comparison of the noise power of the ion beam with and without cooling.

The momentum spread and beam emittance as a function of the number of ions for three species of bare ions stored at an energy of 400 MeV/u are shown in Fig. 4. The momentum spread and the horizontal beam emittance correspond to the 1σ-width of a Gaussian distribution. The momentum spread is derived from the longitudinal distribution obtained by spectral analysis of the Schottky noise. The transverse emittance is calculated from the scraper position which corresponds, according to a comparison with beam profiles, to approxi-

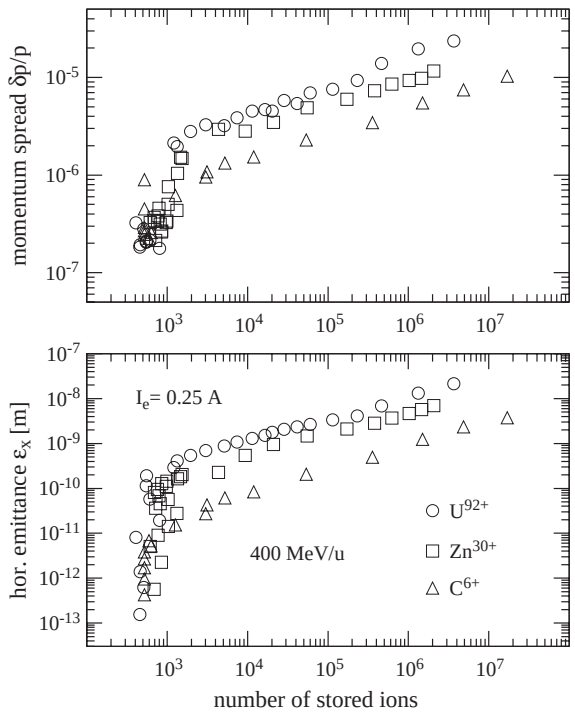

Fig. 4. Comparison of momentum spread and horizontal emittance (1σ-values) for three ions (C^{6+}, Zn^{30+}, U^{92+}) with an energy of 400 MeV/u cooled by an electron current of 0.25 A. For all ions a strong reduction of the momentum spread and of the horizontal emittance at about 1000 stored ions is evidenced indicating the transition to an ordered state.

mately a 3σ-value of the distribution. The emittance $\varepsilon_x = x^2/\beta_x$ finally follows by dividing the square of the 1σ-value of the transverse beam size by the focusing function β_x at the scraper position with $\beta_x = 16$ m.

For all ions momentum spread and emittance increase with intensity when the particle number is larger than about 1000. Around 1000 stored ions a drop of the momentum spread and the horizontal emittance is evident. The momentum spread drops from a value of a few times 10^{-6} in the intrabeam scattering dominated regime to 2×10^{-7}. The emittance reduction is even larger, for U^{92+} the emittance drops from 2×10^{-10} m to about 10^{-13} m below the transition point. The transition seems to be instantaneous without any intermediate regime.

The lowest values for the momentum spread and the horizontal emittance are caused by the resolution of the diagnostics technique. The momentum width of the frequency distribution is broadened by variations of the revolution frequency due to ripple of the main dipole magnet power supplies. The minimum beam radius corresponds to the smallest energy step of $\Delta E/E = 6 \times 10^{-6}$ for the electron beam energy. For all three ions the transition particle number is close to 1000. The reduction factor increases with the charge of the ion. The lower values for the ultra-cold beam are the same for all ions, but the values for constant particle number in the intrabeam scattering dominated regime increase with the ion charge, which results in the larger reduction factor for higher ion charge.

For the lowest measured momentum spreads and horizontal emittances the corresponding temperatures of the ion beam can be calculated. The longitudinal ion beam temperature $kT_{\|} = m_i c^2 \beta^2 (\delta p/p)^2$ and the transverse ion beam temperature $kT_x = m_i c^2 \beta^2 \gamma^2 (\varepsilon_x/\beta_x(s))$ depend on the rest mass $m_i c^2$ of the ion, the Lorentz factors β and γ and on the rms-values of the momentum spread $\delta p/p$ and of the emittance ε_x. The transverse temperature varies with the optical β_x-function along the ring circumference. The values in Fig. 4 multiplied by the ion mass are therefore proportional to the ion temperature. The temperature values above and below the transition point for the ions shown in Fig. 4 are listed in Table 1. It demonstrates the large temperature reduction of the ultra-cold beam. As the measured values of momentum spread and emittance below the transition point are nearly the same for all ion species, the temperature correspondingly scales with the ion mass. Deviations for the transverse temperature below the transition point are due to experimental deficiencies which result in a variation of the minimum detectable beam radius in the range 5–9 μm.

Table 1
Horizontal and longitudinal temperature (in meV) of ion beams above and below the transition to the ultra-cold state

	Above transition		Below transition	
Ion	kT_x	$kT_{\|}$	kT_x	$kT_{\|}$
$^{12}C^{6+}$	5.3	4.0	0.14	0.26
$^{70}Zn^{30+}$	318.0	78.0	1.0	1.5
$^{238}U^{92+}$	1690.0	470.0	0.93	5.0

The transverse ion temperature, which is an average over the whole ring, is much below the transverse electron temperature of 0.1 eV. The effective temperature in the rest frame of the beam must be determined by the longitudinal electron temperature. This is most evident from the very low temperature for carbon beam which in both degrees of freedom is below 0.3 meV.

5. Bunching of ultra-cold beams

The transition to the ultra-cold beam usually starts from the intrabeam scattering dominated regime and results in a temperature reduction when the intensity falls below the threshold value. The transition particle number of about 1000 stored ions cooled by an electron current of 0.25 A corresponds to a maximum line density of 10 ions/m, virtually independent of the ion species. It has been proposed that starting with an ultra-cold beam line densities higher by more than an order of magnitude are achievable in the ultra-cold state [14]. A possibility to start from an ultra-cold beam and increase the line density is the application of RF voltage at an harmonic of the

revolution frequency in order to compress the ions to bunches.

An experiment was performed studying the behavior of an ultra-cold beam of bare uranium at 400 MeV/u when a sinusoidal RF voltage is applied. At the sixth harmonic of the revolution frequency (11.82 MHz) the RF amplitude was adiabatically increased from zero. The longitudinal Schottky signal at the 29th harmonic of the revolution frequency was used as diagnostics. At small RF amplitudes (of a few hundred millivolts) a narrow central line and satellites at the synchrotron frequency were observed. The synchrotron frequency allows a precise determination of the effective RF voltage applied to the beam. With increasing RF voltage the spectral distribution of the Schottky signal changed significantly. At a certain RF voltage the signal amplitude increased by nearly two orders of magnitude and simultaneously a broad distribution developed underneath the narrow central line, indicating the transition from the ultra-cold to the intrabeam scattering dominated regime. This drastic change of the Schottky signal was measured for various particle numbers of the ultra-cold beam (Fig. 5). The maximum RF voltage which does not destroy the ultra-cold beam increased with decreasing particle number.

The length of a bunch can be estimated for a maximum momentum deviation $(\Delta p/p)_{\max}$ according to

$$l_{\mathrm{b}} = 2\frac{c\eta}{\omega_s}(\Delta p/p)_{\max} \tag{1}$$

with the synchrotron frequency ω_{s} for a stationary RF bucket

$$\omega_{\mathrm{s}}^2 = \omega_{\mathrm{rev}}^2 \frac{h\eta q e V_0}{2\pi\beta c p_0}. \tag{2}$$

The synchrotron frequency depends on the revolution frequency ω_{rev}, the harmonic number h, the frequency slip factor η, the ion charge qe, the RF amplitude V_0, the beam velocity βc, and the beam momentum p_0. The line density of the bunched beam can be determined as $N/(hl_{\mathrm{b}})$. The expected dependence of the maximum RF amplitude versus the particle number for a line density of 10 ions/m is indicated in Fig. 5 for a maximum momentum

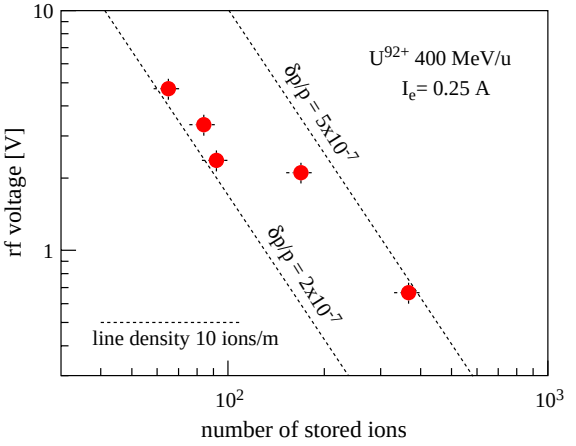

Fig. 5. Limit of the RF voltage which can be applied to the ultra-cold beam before heating is observed as a function of the number of stored ions. A sinusoidal RF voltage at 11.8 MHz is applied to a bare uranium beam at 400 MeV/u which is cooled with an electron current of 0.25 A. The dashed lines show the expected dependence for a constant line density of 10 ions/m and two values of the maximum momentum deviation.

deviation of 2×10^{-7} and 5×10^{-7}. The measured values fall between the two corresponding lines. The difference of the slope in the experimental data can be attributed to the fact, that the bunch length formula is valid, if the momentum spread is small compared to the height of the RF bucket. For small RF amplitudes the ions are not confined longitudinally to the linear part of the RF voltage and the actual bunch length is increased. The momentum spread assumed for the calculation is in good agreement with the measured momentum spread of the coasting ultra-cold beam.

According to the measurement the line density cannot be increased by longitudinal compression of an ultra-cold beam above the value observed for coasting beams. It shows that the line density is basically the quantity which for a certain electron current determines the maximum particle number in the ultra-cold state. It can be concluded that the ultra-cold state, for a given cooling rate, is limited by the line density of the ions. The line density determines the average time between close Coulomb collisions which result in heating by intrabeam scattering. If the longitudinal cooling time is shorter than the average time interval between

Coulomb collisions, the hard Coulomb collisions are suppressed. This is also in agreement with the observation that the threshold particle number of the ultra-cold state increases with the cooling rate provided by the electron beam [12,15].

6. Cooling of decelerated highly charged ions

The availability of decelerated highly charged heavy ions is most important for precision atomic physics experiments in order to reduce Doppler effects which limit the resolution. Electron cooling is employed in the deceleration procedure to prepare a high-quality beam for deceleration and to re-cool the beam after deceleration. The typical deceleration cycle comprises injection and cooling at about 400 MeV/u, deceleration to an intermediate energy of 30 MeV/u with electron cooling and finally further deceleration to the energy requested by the experiment.

The range of beam energies after deceleration could recently be extended to 3 MeV/u, which is the design energy for ESR operation with decelerated beams. This goal was achieved after providing the possibility to ramp not only the magnetic field in the ring magnets, but also the magnetic field of the electron cooling system. At injection energy a minimum magnetic field strength of 70 mT is required for stable electron beam operation, for lower electron energy the magnetic field can be reduced. In previous experiments the magnetic field stayed on the higher value, therefore the closed orbit distortion in the cooling section grew during deceleration and finally resulted in beam loss at the acceptance. By reduction of the magnetic field strength from 80 mT at injection energy to 15 mT after deceleration bare uranium ions were successfully decelerated from 400 MeV/u to a minimum energy of 3 MeV/u. At the lowest energy a maximum of 10^5 ions were detected with a lifetime of 5 s completely determined by interaction with the residual gas. The ions were cooled at 3 MeV/u by an electron current of 5 mA at an electron energy of 1.65 keV. The electron current had to be reduced considerably in order to avoid additional particle losses. The reason of the additional losses is not yet clear. It could be caused by poor quality of the low-energy electron beam confined by a weak magnetic field. More likely are stronger energy variations during cooling with higher electron beam space charge, as the acceptance of the storage ring at the very low magnetic rigidity is small.

Even with the low electron current of 5 mA the beam of 10^5 bare uranium ions was cooled in a few seconds to an emittance $\varepsilon_x = 0.5 \times 10^{-6}$ m and a momentum spread $\delta p/p = 1 \times 10^{-4}$ (2σ-values). Detection was performed as usual by Schottky diagnostics and by detection of residual gas ions with the beam profile monitor. By further optimization of the parameters of the ring and electron cooler it should be possible to increase the number of stored ions after deceleration and to increase the electron current for faster and more powerful cooling.

References

[1] B. Franzke, Nucl. Instr. and Meth. B 24 (1987) 18.
[2] H. Reich, B. Franzke, A. Kritzer, V. Varentsov, Nucl. Phys. A 626 (1997) 417c.
[3] B. Franzke, K. Beckert, H. Eickhoff, F. Nolden, H. Reich, A. Schwinn, M. Steck, T. Winkler, Proceedings of the Sixth European Particle Accelerator Conference, Stockholm, Institute of Physics Publishing, Bristol, 1998, p. 256.
[4] M. Steck, K. Beckert, P. Beller, B. Franczak, B. Franzke, F. Nolden, U. Popp, A. Schwinn, Phys. Scripta T104 (2003) 64.
[5] F. Nolden, K. Beckert, P. Beller, B. Franzke, C. Peschke, M. Steck, Nucl. Instr. and Meth. A, (2004) these Proceedings.
[6] N. Angert, W. Bourgeois, H. Emig, B. Franzke, B. Langenbeck, K.D. Leible, T. Odenweller, H. Poth, H. Schulte, P. Spädtke, B.H. Wolf, Proceedings of the Second European Particle Accelerator Conference, Nice, Editions Frontières, Gif-sur-Yvette, 1990, p. 1374.
[7] P. Beller, K. Beckert, B. Franzke, C. Kozhuharov, F. Nolden, M. Steck, Nucl. Instr. and Meth. A, (2004) these Proceedings.
[8] M. Steck, K. Beckert, H. Eickhoff, B. Franzke, F. Nolden, P. Spädtke, Proceedings of the 1993 Particle Accelerator Conference, Washington DC, 1993, p. 1738.
[9] M. Steck, Nucl. Phys. A 626 (1997) 473c.
[10] M. Steck, K. Beckert, F. Bosch, H. Eickhoff, B. Franzke, O. Klepper, R. Moshammer, F. Nolden, H. Reich, B. Schlitt, P. Spädtke, T. Winkler, Proceedings of the Fourth European Particle Accelerator Conference, London, 1994, p. 1197.

[11] M. Steck, Proceedings of 255th International WE-Heraeus-Seminar on Beam Cooling and Related Topics, Bad Honnef, Forschungszentrum Jülich (ISBN 3-89336-316-5, ISSN 1433-5506), 2002.
[12] M. Steck, K. Beckert, H. Eickhoff, B. Franzke, F. Nolden, H. Reich, B. Schlitt, Phys. Rev. Lett. 77 (1996) 3803.
[13] M. Steck, K. Beckert, P. Beller, B. Franzke, F. Nolden, J. Phys. B, At. Mol. Opt. Phys. 36 (2003) 991.
[14] R.W. Hasse, Phys. Rev. Lett. 83 (1999) 3430.
[15] H. Danared, A. Källberg, K.-G. Rensfelt, A. Simonsson, Phys. Rev. Lett. 88 (2002) 174801-1.